Survey of Sky EffectiveTemperature Models Applicable to Building Envelope Radiant Heat Transfer

2 **authors**, including:

Salem Algarni
King Khalid University

7 PUBLICATIONS   **9** CITATIONS

SEE PROFILE

Survey of Sky Effective Temperature Models Applicable to Building Envelope Radiant Heat Transfer

Salem Algarni
Student Member ASHRAE

Darin Nutter, PhD, PE
Fellow ASHRAE

ABSTRACT

Radiative sky cooling is a result of heat loss by longwave emission toward the sky. For the use in heat transfer applications and calculations, researchers have studied and proposed different sky effective temperature models and correlations since the early 1900s. One such use is for calculating a building's cooling loads, where the sky longwave exchange is an effective building energy balance element. Several factors influence the effective sky temperature, including location, ambient temperature, dew point temperature, and cloud cover. As a result, knowledge of current sky temperature models is important to better understand and characterize building heat transfer interactions, i.e., sky longwave radiative exchange. Therefore, the objective of this paper is to provide a comprehensive survey of existing sky temperature models from the available literature. The role of sky radiative exchange within building energy calculation is demonstrated. Moreover, the models are categorized by data input requirements and wide-ranging results are shown under various climate conditions. Finally, for selected models, a comparison of hourly sky radiation exchange from a horizontal surface is provided.

INTRODUCTION

During summertime conditions, heat gain through a building's exterior surface includes various forms of absorbed incident solar radiation, long wavelength radiation exchange, and absorbed heat via convection. For many years, the conventional method to account for these three energy interactions has been to incorporate an effective outdoor air temperature known as the *sol-air* temperature (Kuehn et al. 1998; ASHRAE 1989). Under this method, the radiative exchange between a building's external surfaces and the sky, also known as the *sky longwave radiation exchange*, is simplified through the use of linearized radiation coefficients and a constant effective sky temperature correction factor. Similarly, current building energy simulation software programs use simple empirical models to predict the sky effective temperature and radiation exchange. Of singular interest in this paper is the current knowledge of modeling the sky effective temperature.

The sky longwave radiation exchange is mainly a function of the sky effective temperature. In particular, radiative cooling is a result of heat loss by longwave radiation emission toward the sky, where the sky can be used as a heat sink for exterior surfaces of buildings. Radiative cooling is largest (i.e., the effective sky temperature is the lowest) at night when the sky is clear and humidity is low. Clouds trap heat and increase the sky temperature (Saitoh and Fujino 2001). On a clear night, a building's external surface temperatures typically drop below the ambient temperature due to heat loss to the sky. In fact, recently the night-sky cooling phenomenon has motivated applications such as thermal collectors, movable insulations, and air-water roof radiators through experiments and theoretical investigations. Eicker and Dalibard (2011) developed a new thermal collector for the night cooling of buildings in central Spain that provides a cooling power of 42.5 W/m^2 (12.7 Btu/hr·ft^2). Cavelius et al. (2005) claimed that the night sky can provide cooling power in the range of 20–80 W/m^2 (6.3–25.4 Btu/hr·ft^2). For predictions, accurate estimations of the sky temperature are critical. For example, at midlatitude sites, it has been reported that a 5% error of estimating the sky longwave radiation may represent 20 W/m^2 (6.3 Btu/hr·ft^2) (Berdahl and Fromberg 1982). As a result, predictions of sky temperature have been an interest for many investigators.

Salem Algarni is a PhD candidate and **Darin Nutter** is a professor in the mechanical engineering department, University of Arkansas, Fayetteville, AR.

Researchers have studied and proposed numerous sky effective temperatures models since the early 1900s. Most of these sky temperature models are proposed in an approximated manner due to the lack of accurate measured data (Martin and Berdahl 1984). Poor agreements are expected because these sky models are related to local weather conditions and specific sites, as well as difficulty in finding reliable measured data. Therefore, variations between the sky temperature models have been a motivation for developing new sky models for different locations over the years (Tang et al. 2004). Furthermore, success of several radiant systems in residential buildings has attracted researchers for generating an accurate database of atmospheric radiation (Clark and Allen 1978). In general, the current sky models are developed based on local weather and site locations and, unfortunately, do not cover much of the world.

Although the use of the sol-air model is defined to give approximated results (Spitler 2010), the model does not account for variations with time, the effect of cloudiness, dust or different locations. In fact, cloud cover has a strong influence on sky radiation (Mills 1995). Since individual models are limited to certain weather conditions and specific sites, each model may not apply for different sites and climate conditions. Furthermore, several studies have been performed on thermal buildings' performances without careful consideration of sky radiation effect. Very simple approximations for the longwave radiation between the sky and the buildings' surfaces have been used. For example, the sky temperature was assumed to be 12°C or 6°C (21.6°F or 10.8°F) below ambient temperature for daily calculation (Al-Sanea 2000; Praëne et al. 2005). Other studies limited the radiation cooling on buildings to the temperature difference between the buildings' surface and ambient temperature (Khedari et al. 2000; Chesné et al. 2011). However, in a recent a study, the difference between the ambient and the sky temperature in desert areas can reach 25°C (45°F) (Twidell and Weir 2005).

To better quantify the influence of sky longwave radiation exchange on a building's external surface, an accurate sky effective temperature should be considered. Therefore, this paper provides a comprehensive review of existing sky temperature models, both clear and cloudy, from the available literature. The models were categorized by data input requirements and computational approaches. The model results were demonstrated under various climate conditions. Finally, for selected models, a comparison of hourly sky radiation exchange from a horizontal surface is provided.

HEAT TRANSFER MECHANISMS WITHIN BUILDING HORIZONTAL SURFACES

A composite horizontal surface (roof) of multiple layers M is shown in Figure 1. The roof's outside surface is exposed to outside convection heat flux (q_{conv}), solar absorbed (q_{abs}), and sky longwave radiation exchange (q_{sky}). The inside surface of the composite roof is subjected to combined internal convection and radiation heat transfer (q_i). All these parame-

ters vary with time of day, month of year, and location. Therefore, the heat transfer characteristic across the roof is considered a transient heat transfer phenomenon. During a clear sky night, the net heat transfer balance is negative (cooling) due to the longwave radiation between the roof and the sky. In other words, the roof is losing heat to the sky. However, during the daytime, the net heat transfer balance is positive (heating) because of the dominance of incident radiation on the solar radiation exchange. Note that for a nonhorizontal surface, calculating the effective sky temperature requires a path length (McQuiston et al. 2005).

The longwave radiation exchange between the sky and a building roof surface can be estimated as follows:

$$q_{sky} = \varepsilon\sigma F_{SS}(T_{sky}^4 - T_{x=L}^4) \qquad (1)$$

where the sky view factor with respect to flat roof equals 1.

As an example, Figure 2 shows results from modeling a horizontal roof's heat transfer components and variation on July 21 for the hot-dry climate and clear sky conditions of Phoenix, AZ. The heat transfer components were calculated numerically by using the implicit finite difference method (Al-Sanea 2002). In the model, the ambient air temperatures are sinusoidal averaged for the day (McQuiston et al. 2005). The ambient air temperature used was 40.15°C (maximum) and 27.32°C (minimum) (104.3°F and 81.2°F, respectively) (NOAA 2014). The incident total solar radiation on the horizontal roof was calculated by using the ASHRAE clear sky model (ASHRAE 2013) for the latitude and longitude of Phoenix, AZ. Garg's (1982) model was used to predict the sky temperature. In the simulation, the roof consists of 150 mm (5.9 in.) of reinforced concrete and a layer of plaster attached to the inside of the
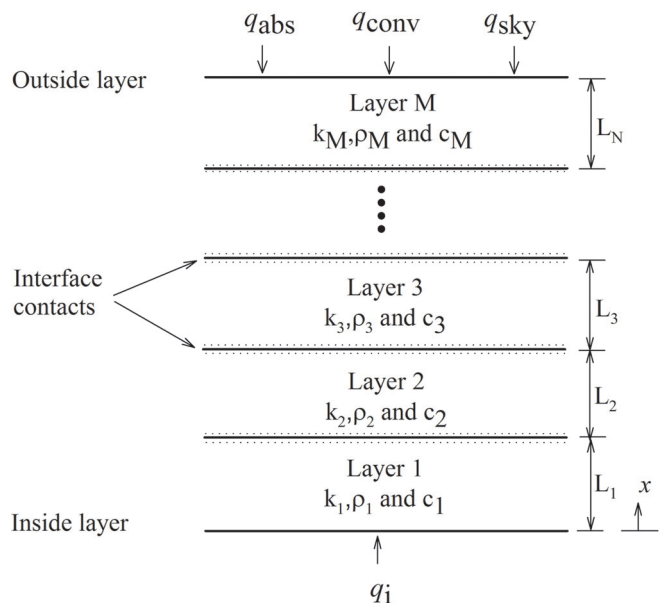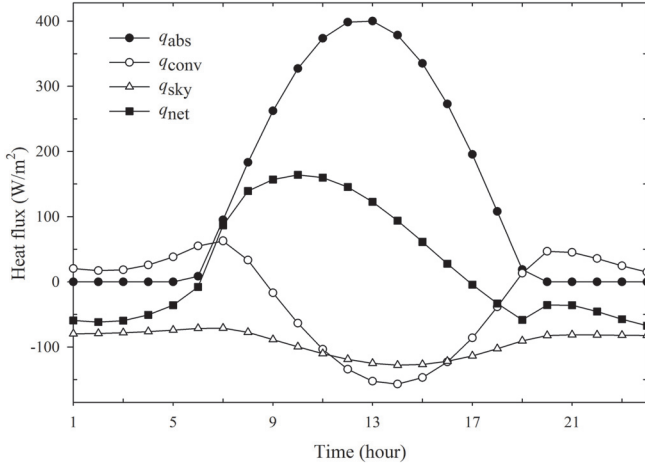

Figure 1 *A composite roof with multiple layers* M.

Figure 2 *The roof's heat transfer components at various times of day on July 21 for the hot-dry climate and clear sky conditions of Phoenix, AZ.*

roof was selected. Thermophysical properties of the roof materials were given by Al-Sanea (2000).

During daylight hours, the solar absorbed (q_{solar}) is the dominant heat gain onto the surface. On the other hand, the sky longwave radiation (q_{sky}) contributes as a cooling source for buildings, as long as the sky temperature is lower than the ambient temperature. The outside roof convection (q_{conv}) heat transfer is the result of the difference between the outside roof and ambient temperature difference.

As shown in Figure 2, q_{sky} represents a large portion of the roof cooling load which helps reduce the total heat gain over the course of the day. This example demonstrates the potential importance of accounting for sky cooling, a strong function of the sky temperature. Analysis of heat transfer components for different climatic locations result in similar profiles with varying amplitude. As would be expected in cooler climates, the longwave sky cooling may be minimized.

SKY TEMPERATURE MODELS CLASSIFICATIONS

The sky temperature is unlike the ambient air temperature. In general, the effective sky temperature is always lower than the ambient air temperature due to a decrease in elevation (Mills 1995). In addition, the difference between ambient air temperature and sky temperature is higher in the summer months, especially under clear sky conditions. Because of the water vapor and carbon dioxide heat absorption in cloudy sky conditions (Berdahl and Fromberg 1982), clouds usually increase the effective sky temperature causing it to approach the ambient air temperature. Moreover, the effective sky temperature depends on many factors such as ambient temperature, dew point, amount of clouds, and the site conditions. Therefore, these factors have to be considered when developing sky temperature models.

Within the literature, there are several sky temperature models and emissivity correlations that have been proposed to estimate the effective sky temperature. Most of these models apply to clear sky conditions. Other models use correction factors to account for average cloud cover. The effective sky or atmospheric temperature can be related to ambient air temperature by using the following equation (Centeno 1982):

$$T_{sky} = (\varepsilon_{sky})^{0.25} T_{amb} \qquad (2)$$

Estimating the sky temperature can be classified within three main methods: empirical methods, radiation charts and detailed methods. Empirical methods are based on measurements and collected atmospheric data. Radiation charts are based on theoretical or empirical radiation calculations to generate a minimum, mean and maximum monthly sky temperature in chart formats (Cole 1976). Detailed methods, on the other side, are computer program models that utilize very detailed atmospheric constituents (Berdahl and Fromberg 1982). These kinds of computer programs require very detailed inputs and are considered time consuming similarly radiation charts methods. Therefore, the focus in this study is on the empirical methods.

In empirical methods, sky models can be divided into two groups: clear and cloudy sky models. Each of these models can be classified into direct sky temperature models and atmospheric emissivity correlations. Associated with atmospheric emissivity correlations, Equation 2 should be used to calculate the effective sky temperature as a function of local ambient air temperature. Figure 3 represents a classification of effective sky temperature models and their dependent parameters.

For clear sky models, Table 1 lists the available atmospheric emissivity correlations. In general, these atmospheric emissivity algorithms are essentially functions of the dew point temperature (Models 1–11) and a few of water vapor partial pressure (Models 12–18). Moreover, some investigators have provided specific emissivity sky models for nighttime and others for daytime sky temperature (Models 1–2 and 4–5). Emissivity correlations models from Table 1 are discussed below.

- **Berger et al. (1984)** developed two separate models (1 and 2) to predict daytime and nighttime sky emissivity. The two models were based on five years' measurements and analysis at Carpentras, France through January 1976 to December 1980. In the model by Berger et al., measurements of sky radiation fluxes were taken for every 3 hours and then integrated hourly for 859 daytime and 750 nighttime measured data points. The root mean square error over T_{sky} is 2.7°C (4.9°F).
- **Tang et al. (2004)** developed another nighttime emissivity correlation based on a short period of time (August 10–October 25, 2002) for the climate of Negev Highlands, Israel. The model is valid for a narrow range of ambient temperatures, between 19°C to 33.5°C (66.2°F
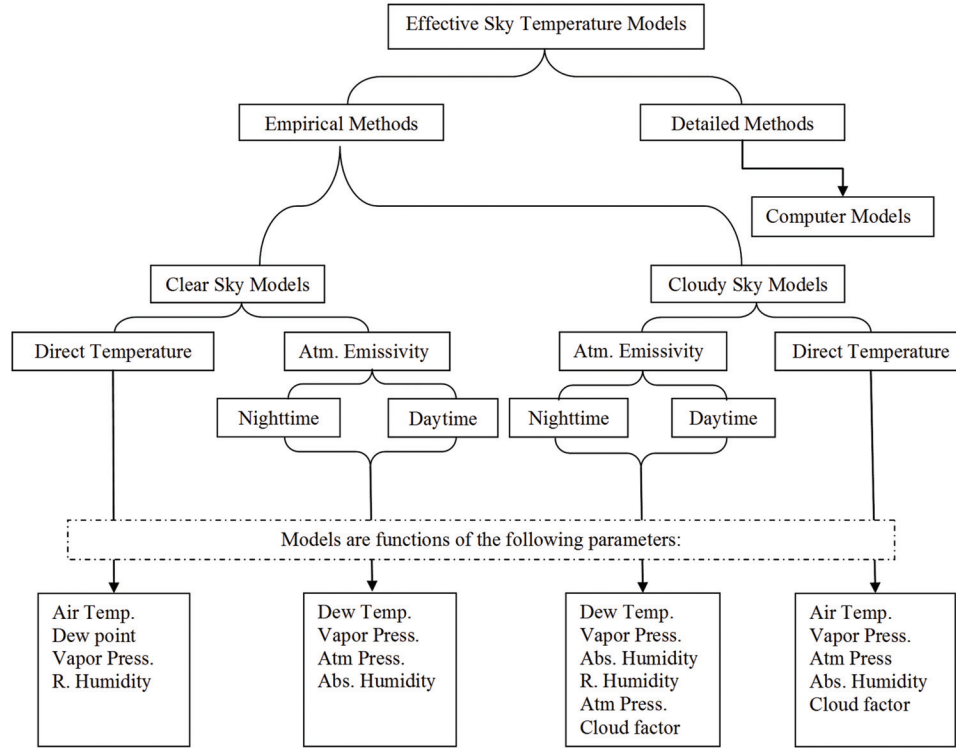
Figure 3 *Sky temperature models classifications.*

to 92.3°F) and average relative humidity of 26% to 90%. The method of open pond temperature variation and radiation exchange with sky, at nighttime, is used in the model to develop the correlation. The method is considered simple in comparison to other models' methods, where direct hourly measurements of sky longwave radiation fluxes are used. Furthermore, the model is not recommended for very hot, dry climates. The standard deviation of sky emissivity for a linear regression that was reported in Tang et al.'s emissivity model is 0.051.

- **Berdahl and Fromberg (1982)** presented two models for day- and nighttime clear sky emissivity. The measurements of longwave radiation were collected during 11 summer months in 1979 for three different U.S. locations: Tucson, AZ, Gaithersburg, MD and St. Louis, MO. The reported standard error was 0.031. Berdahl and Fromberg noticed that the average daytime sky emissivity is lower than the average nighttime sky emissivity by 0.016. In general, since the model is based on summer collected data, it may not be applicable for other weather conditions. Later, a set of 57 months of sky longwave radiation data was collected by Berdahl and Martin (1984) for six U.S. sites to develop a new model with better accuracy. These sites were Tucson, AZ; San Antonio, TX; Gaithersburg, MD; St. Louis, MO; West Palm Beach, FL; and Boulder City, NV. Compared to the old model, the effect of the site on the

sky emissivity was notable. The new model showed that Gaithersburg, MD has a higher sky emissivity than the rest of the other sites by an average of 0.019. The new model was recommended to be used for the range of $-13 \leq T_{dp} \leq 24°C$ ($8.6 \leq T_{dp} \leq 75.2°F$).

- **Bliss (1961)** presented analytical procedures for calculating the clear sky emissivity. In addition, Bliss used water vapor emissivity measurements by Hottel and Egbert (1942) and Kondratyev (1969) to develop Bliss' sky model. The range of the dew point in the model is $-20 < T_{dp} < 30°C$ ($-4 < T_{dp} < 86°F$). However, the calculated sky emissivity is always higher than the measured emissivity.

- **Chen et al. (1991)** measured 150 nights of data in order to develop the dew point sky emissivity model. The model was based on data collected in Omaha, NE and Big Bend, TX. The variation between the results of Clark and Allen and Berdahl and Fromberg were the motivation of Chen et al.'s (1991) work. The results of the model agree with Berdahl and Fromberg's model. The model's root square error is 0.588. In 1995, Chen et al. (1995) collected a larger set of data with more than 1400 points to develop a better fit model. The result of the new model is within 2% difference with Berdahl and Fromberg (1982) and 7% difference with Clark and Allen (1978). The range of dew point in the new model is $0 < T_{dp} < 30°C$ ($32 < T_{dp} < 86°F$). Therefore, Chen et

Table 1.   Clear Sky Atmospheric Emissivity Models

	Model	Site	Author/Reference
1	$\varepsilon_{sky} = 0.77 + 0.0038 T_{dp}$	Carpentras, France	Berger et al. (1984)
2	$\varepsilon_{sky} = 0.752 + 0.0048 T_{dp}$		
3	$\varepsilon_{sky} = 0.754 + 0.0044 T_{dp}$	Negev Highlands, Israel	Tang et al. (2004)
4	$\varepsilon_{sky} = 0.741 + 0.0062 T_{dp}$	AZ/MD, and MO	Berdahl and Fromberg (1982)
5	$\varepsilon_{sky} = 0.727 + 0.0061 T_{dp}$		
6	$\varepsilon_{sky} = 0.711 + 0.56(T_{dp}/100) + 0.73(T_{dp}/100)^2$	AZ, TX, MD, MO, FL, NV	Berdahl and Martin (1984)
7	$\varepsilon_{sky} = 0.8004 + 0.00396 T_{dp}$	AZ	Bliss (1961)
8	$\varepsilon_{sky} = 0.8 + T_{dp}/250$		
9	$\varepsilon_{sky} = 0.736 + 0.00577 T_{dp}$	Omaha, NE Big Bend, TX	Chen et al. (1995)
10	$\varepsilon_{sky} = 0.732 + 0.00635 T_{dp}$		Chen et al. (1991)
11	a. $\varepsilon_{sky} = 0.787 + 0.764 Ln(T_{dp}/273)$ b. $\varepsilon_{sky} = 0.787 + 0.0028 T_{dp}$	San Antonio, TX	Clark and Allen (1978) Clark et al. (1985)
12	$\varepsilon_{sky} = 0.56 + 0.08\, P_v^{0.5}$	Los Chorros, Macuto, Caracalleda, Maracaibo, and Mérida, Venezuela	Melchor (1982a)
13	$\varepsilon_{sky} = 0.48 + 0.058\, P_v^{0.5}$	Bassour, Algeria	Angstrom (1918)
14	$\varepsilon_{sky} = 0.50 + 0.032\, P_v^{0.5}$	Whitney, CA	
15	$\varepsilon_{sky} = 0.62 + 0.029\, P_v^{0.5}$	Poona, India	Raman (1935)
16	$\varepsilon_{sky} = 0.34 + 0.110\, P_v^{0.5}$	Lindenberg, Germany	Robitzsch (1926)
17	$\varepsilon_{sky} = (0.135 \times P_{atm} + 6 P_v)/T_{amb}$		
18	$\varepsilon_{sky} = 0.7 + 5.95 \times 10^{-5} \times P_v e^{(1500/T_{amb})}$	Phoenix, AZ	Idso (1981)
19	$\varepsilon_{sky} = 0.3714 + 0.01923 \times AH$	Columbus, OH	Sloan et al. (1956)

al.'s (1991) model is not recommended to apply in such a site where the dew point is below 0°C (32°F).

- **Clark and Allen (1978)** collected 800 measurements of nocturnal net radiosity of the sky from October of 1976 until September 1977 at Trinity University, San Antonio TX. As a result of the observations, the night sky emissivity correlation was developed with an error of 10 W/m^2 (3.2 Btu/hr·ft^2). The absence of accurate long-term related atmospheric data at that time could be the result of the error. The model can be used for dew point temperatures in the range of –20.2°C to 24.5°C (–4.4°F to 76.1°F). Based on the instrument's measurement accuracy at the time, the reported error was stated as "small."

- **Melchor's (1982a)** measurements were carried out in Venezuela. The model is applicable for ambient temperatures between –10.2°C and 29.9°C (13.6°F and 85.8°F) and relative humidity range of 40%–100%. The valid elevation that can be used in this model is from 0 to 3000 m (0 to 9842.5 ft).

- **Angstrom's (1918)** model is considered one of the earliest works that attempted to predict the sky emissivity. The model was developed by a long series of observations and is only a function of the actual atmospheric vapor pressure in millibars. Angstrom developed the model using measurements at Bassour, Algeria at an elevation of 1160 m (3805.8 ft) and later at Mt. Whitney, CA at an elevation of 2860 m (9383.2 ft). Many investigators developed their models using Angstrom formula structure with only modified coefficients, such as Robitzsch (1926), Raman (1935), and Melchor (1982a).

- **Idso (1981)** used one year's worth of measurements to evaluate this sky emissivity model. The model is valid for ambient temperatures of $-5.2 \leq T_{amb} \leq 40.9$°C (22.7 $\leq T_{dp} \leq 105.6$°F) and vapor pressures within $30 \leq P_v \leq 3000$ Pa ($0.4 \leq P_v \leq 435.1$ psi).

- **Sloan et al. (1956)** developed a model as a function of absolute humidity only. The measurements were taken for the two years of 1954–1956 in Columbus, OH.

On the other hand, two clear sky direct temperature models are summarized in Table 2. Swinbank (1963) averaged the elevation and the humidity values and proposed a direct sky model as a function of ambient air temperature. Garg (1982) evaluated the sky temperature as 20°C (36°F) below the ambient temperature based on measured data in Australia. Though these models are fairly simple, associated errors are expected.

Finally, the impact of cloudiness on sky temperature is difficult to evaluate, and only a few researchers have attempted to predict it. Recently, a complete set of weather files covering 3012 international locations outside the United States and Canada has been released as the typical meteorological year (IWEC2) format (Huang et al. 2014). The new set of weather data includes values for hourly opaque and total cloud cover. The cloud cover data are necessary for building simulation programs to better predict the sky temperature under cloudy sky conditions. In Table 3, the cloud atmospheric emissivity correlations were introduced by the following authors:

- **Kasten and Czeplak (1980)** introduced a cloudiness factor (C_{cover}) that can take values between 0 (for clear

sky) and 1 (for totally cloudy sky). The model was based on hourly sky heat flux measurements that were taken for 10 years (1964–1973) during the daytime. Kasten and Czeplak's study is based on long-term collected hourly data of solar and terrestrial radiation to calculate the effect of cloudiness.

- **Melchor (1982b)** developed another model from the exploration of several measurements that have been taken by other investigators in the United States, France, India, England, Germany, and Sweden. The model is valid for the same range of weather conditions as stated in Melchor's (1982a) clear sky emissivity model. In addition, Melchor's (1982b) model is a detailed model that accounts for several factors: ambient air temperature, site elevation, relative humidity, and degree of cloudiness. In the model, the degree of cloudiness ranges between 1 for very cloudy and 0 for clear sky conditions. Due to the large number of variables incorporated by Melchor's (1982b) model, it is considered more comprehensive than others.

- **Berdahl and Martin (1984)** introduced a cloud sky fraction (f_{cloud}) to account for the cloudiness effect. In case of clear sky conditions, the cloud sky fraction is zero and one for overcast sky. Berdahl and Martin used the same data as in Berdahl and Fromberg's (1982) model to explore the effect of cloudiness. In the model, cloudiness emissivity was assumed to be 0.9. In general, Berdahl and Martin's (1984) model is similar to Kasten and Czeplak's (1980) model.

Table 2. Clear Sky Direct Temperature Models

	Model	Site	Author/Reference
20	$T_{sky} = T_{amb} - 20$	Australia	Garg (1982)
21	$T_{sky} = 0.0552\, T_{amb}^{1.5}$	Australia	Swinbank (1963)

Table 3. Cloudy Sky Atmospheric Emissivity Models

	Model	Site	Author/Reference
22	$\varepsilon_{sky} = \varepsilon_{sky\text{-}clear} + 0.8(1 - \varepsilon_{sky\text{-}clear})C_{cover}$	Hamburg, Germany	Kasten and Czeplak (1980)
23	$\varepsilon_{sky} = (1 - N) \times [57.723 + 0.9555(0.6017)^Z] \times 10^{-4} \times T_{amb}^{1.1893} \times H^{0.0665} + N[1 - (3000 + 1751 \times Z^{0.652}) \times H^{-3/2} \times T_{amb}^{-1}]^4$	Los Chorros, Macuto, Caracalleda, Maracaibo, and Mérida Venezuela	Melchor (1982b)
24	$\varepsilon_{sky} = \varepsilon_{sky\text{-}clear} + \varepsilon_{cloud}(1 - \varepsilon_{sky\text{-}clear})f_{cloud}$	AZ, TX, MD, MO, FL, NV	Berdahl and Martin (1984)
25	$\varepsilon_{sky} = 0.682 + 0.0352 \times \ln(P_v) + 0.133 \times \ln(1 - K_0)$	Gembloux, Belgium	Aubinet (1994)
26	$\varepsilon_{sky} = C_a \varepsilon_{sky};$ $C_a = 1 + 0.0224N - 0.0035N^2 + 0.00028N^3$	San Antonio, TX	Clark and Allen (1978)
27	$\varepsilon_{sky} = (0.53 + 0.065. P_v^{0.5})(1 - 0.1N) + 0.1N$	Benson, England	Daguenet (1985)
28	$\varepsilon_{sky} = (0.43 + 0.082. P_v^{0.5})(1 - 0.1N) + 0.1N$	Upasala, Sweden	
29	$\varepsilon_{sky} = (0.44 + 0.061. P_v^{0.5})(1 - 0.1N) + 0.1N$	Washington, DC	
30	$\varepsilon_{sky} = (0.62 + 0.029. P_v^{0.5})(1 - 0.1N) + 0.1N$	Poona, India	

- **Aubinet's (1994)** measurements were carried out at Gembloux, Belgium. The model is a result of measurements that were taken for 274 days (1992–1993). The mean square error between calculated and measured data of daily mean infrared sky radiation (as defined by sky emissivity model 26) is 92 W/m^2 (29.2 Btu/hr·ft^2). In the model, the clearness index (K_0) was used as an indicator for the effect of average cloud cover.
- **Clark and Allen (1978)** estimated the effect of cloud cover by developing a cloud correction factor (C_a). The cloud correction factor is defined as the ratio of measured cloud sky atmospheric radiation to estimated clear sky atmospheric radiation. The formula of the correction factor is a function of opaque sky cover (N) where N equals 0 for clear sky and 10 for overcast sky. The model is valid for the same range of weather conditions as Clark and Allen's clear sky emissivity model.

Other investigators studied the effect of cloud cover on longwave radiation between building surfaces and the sky. Cloudy sky direct temperature models are summarized in Table 4. These models are also briefly discussed below:

- **Dreyfus (1960)** introduced the simplest of the direct sky temperature models. Dreyfus assumed that the sky effective temperature is equal to the ambient temperature in the case of extreme cloudy sky conditions.
- **Whillier (1967)** proposed a similar model where the temperature of the sky was assumed to be 6°C (10.8°F) below the ambient. In both models, neither cloudiness effect nor site conditions were considered.
- **Fuentes (1987)** modified Swinbank's model of clear sky to account for the average cloudy sky by using a clearness

index of 68 cities in the United States. Fuentes used the overall clearness index of 0.61. In addition, Fuentes assumed that cloudiness and sky insolation causes the sky temperature to be 32% closer to the ambient air temperature than Swinbank's (1963) model.

- **Aubinet (1994)** introduced a cloudy sky direct model based on the same data as his model of cloudy sky atmosphere emissivity. However, the mean square error between calculated and measured data of daily mean infrared sky radiation (as defined by sky temperature model 35) is 71 W/m^2 (22.5 Btu/hr·ft^2).Therefore, the Aubinet (1994) model for cloudy direct sky temperature is more accurate than Aubinet's (1994) model of cloud-sky atmospheric emissivity. In the model, the sky clearness index (K_t) was introduced and defined as the ratio between global solar horizontal radiation and extraterrestrial solar radiation.
- **Daguenet (1985)** developed complicated formulas where the effect of ambient temperature, vapor pressure and the emissivity of the sky were considered, in addition to cloudiness degree (N). A value of 8 represents clear sky and 0 for cloudy sky. Note that the model is not very sensitive to the degree of cloudiness.

SKY TEMPERATURE MODELS VARIATIONS

In order to explore the variation between the sky temperature models, both the direct sky temperature and atmospheric emissivity models were analyzed and compared to ambient air temperature. Weather conditions, such as ambient air temperature and dew point temperature for a 24 hour period in Al-Madinah, Saudi Arabia, were used as inputs for the sky models. The ambient air temperatures were sinusoidal averaged for the day (McQuiston et al. 2005). The ambient air temperature used was 43.33°C

Table 4.   Cloudy Sky Direct Models

	Model	Site	Author/Reference
31	$T_{sky} = T_{amb}$	—	Dreyfus(1960)
32	$T_{sky} = T_{amb} - 6$	United States	Whillier (1967)
33	$T_{sky} = 0.037536\,T_{amb}^{1.5} + 0.32 T_{amb}$	68 U.S. sites	Fuentes(1987)
34	$T_{sky} = 94 + 12.6\ln(P_v) - 13K_t + 0.341 T_{amb}$	Gembloux, Belgium	Aubinet (1994)
35	a. $T_{sky} = \left(\dfrac{L}{\sigma}\right)^{0.25}$ b. $L = L_0(1 + 0.01A) + \dfrac{BC(8-N)}{8}$ c. $L_0 = 3.6(T_{amb} - 273) + 231$ d. $A = 10.1\ln(P_v) - 12.3$ e. $B = 1.7(T_{amb} - 273) + 107$ f. $C = -0.22\ln(P_v) + 1.25$	Various international sites	Daguenet (1985)

(maximum) and 30.50°C (minimum) (110°F and 87°F, respectively) (MEPA 2013). The variations between the models can be a result of model limitations and the accuracy of collected data. A comparison of the four sets of sky temperature models are classified and presented in sections that follow.

Clear Sky Atmospheric Emissivity Models

Figure 4 illustrates a comparison between clear sky atmospheric emissivity models and the ambient temperature for a 24 hour period. In general, the comparison shows that the sky temperature can be cooler than the air temperature by 40°C (72°F), as estimated by Angstrom's (1918) United States model. On the other hand, Clark and Allen's (1978) model predicts the highest sky temperature to be 18°C (32.4°F) below the air temperature. Although both models by Angstrom and Clark and Allen were based on measurements in the United States, they represent the two most extreme models. The rest of the clear sky emissivity models fall between the models by Angstrom (1918) and Clark and Allen (1978). Robitzsch (1926) predicted a similar sky temperature in Germany compared to Angstrom's (1918) Algeria model results. The two models of Berger et al. (1984) for day and nighttime were combined and the results presented in one curve. The nighttime emissivity of Berger et al. (1984) in the combined model led to lower sky temperatures during the night. Finally, for the rest of the models, the average sky simulated results were predicted to be around 20°C (36°F) below ambient air temperature.
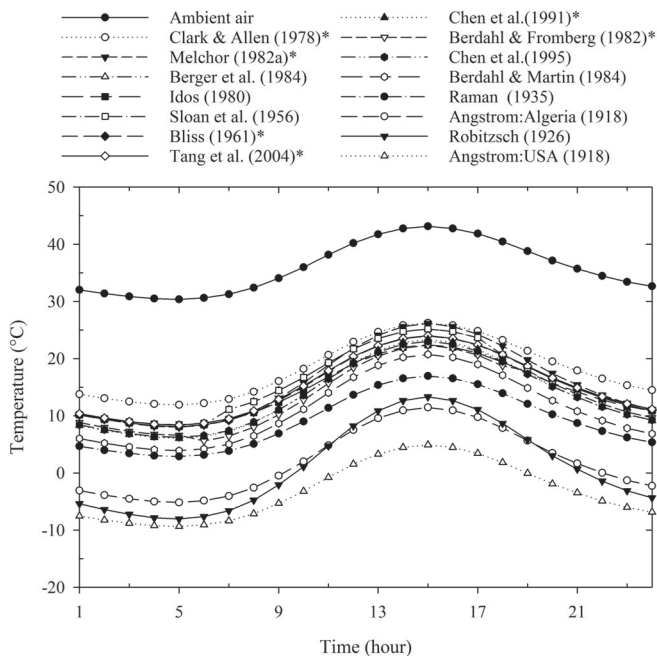
Clear Sky Direct Temperature Models

Garg's and Swinbank's simulation results are presented in Figure 5. The sky temperature is estimated to be lower by Garg (1982), who simply assumed that the sky temperature is 20°C (36°F) below the air temperature. Swinbank's (1963) model shows that the sky temperature drops by 5°C (9°F) at midday and 10°C (18°F) at midnight below the air temperature.

Cloud Sky Emissivity Models

Variation between cloudy sky emissivity models is shown in Figure 6. For average cloudy sky conditions, the estimated sky temperatures can fall between 20°C (36°F) below the air temperature, as estimated by Daguenet's (1985) United States model, and 10°C (18°F) below the air temperature, as predicted by Berdahl and Martin's (1984) model.

Cloud Sky Direct Models

Figure 7 shows the variations of cloudy sky direct models compared to the ambient air temperature. Aubinet's model gave the lowest estimate for sky temperature, around 29°C (52.2°F) below the ambient temperature. As stated earlier, Dreyfus assumed that cloudy sky temperature is the same as air temperature. As a result, Dreyfus's (1960) model is considered to be the highest approximation for the sky temperature in the literature. Whillier (1967) and Fuentes (1987) predicted similar sky temperature for several cities in the United States, however, Fuentes predicted larger differences between sky and ambient temperatures early in the day and smaller differences during the afternoon hours. Daguenet's (1985) detailed model estimated the average cloudy sky to be slightly higher than Aubinet's (1994) prediction.
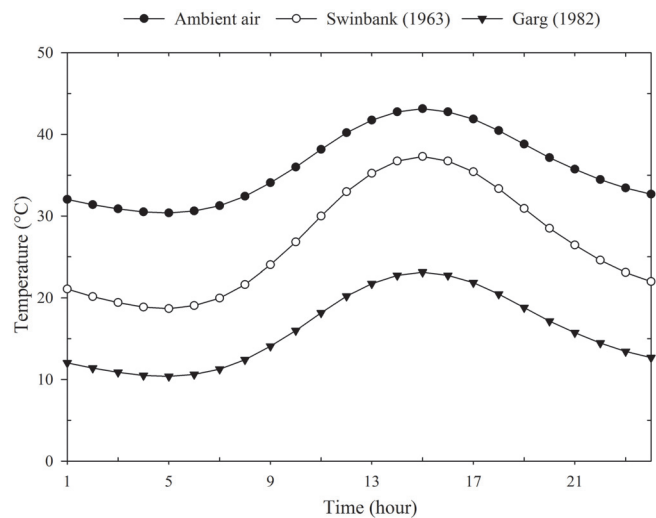

Figure 4 *Computed sky temperatures and comparison of hourly variations between clear sky emissivity models and measured ambient air temperature over a 24-hour period.*

Figure 5 *Comparison of hourly variations between clear sky direct temperature models and measured ambient air temperature over a 24-hour period.*

CLIMATES EFFECT ON SKY MODELS PREDICTION

Because there are few locations with a representative sky temperature model, the literature leads to varying results. To demonstrate the effect of climates on available sky temperature models outside their assigned uses, four general climate conditions were chosen. These climates are: extreme hot-dry, hot-dry, hot-humid, and moderate. Corresponding sites with July maximum and minimum ambient air and dew point temperatures are listed in Table 5.

Three sky temperature models, Melchor (1982a), Melchor (1982b), and Aubinet (1994), were selected and tested under each climate. Results of the tests are discussed below and shown in Figures 8, 9, 10, and 11 for extreme hot-dry, hot-dry, hot-humid, and moderate climates respectively.

The Melchor (1982a) model for clear sky is a solo function of vapor pressure. For hot-humid climates, the model predicted a higher sky temperature where it reaches the ambient temperature at midday. The result was not expected. In the literature, the sky temperature only reaches ambient air temperature in the case of very cloudy conditions. Therefore, the model over predicted

results can be expected in very humid climates. In hot-dry and moderate climates, the model gave higher readings compared with the other two models. Under a hot-dry climate, the differences between the Melchor (1982a) model and ambient temperatures are twice the value in the morning than that during late hours due to low dew point temperatures.

The Melchor (1982b) model expected minimum sky temperature in both hot-humid and moderate climates. On the other hand, in a very hot-dry climate, the model fails to predict similar results in both climates, as shown in Figures 8 and 9. However, the model expected very low sky temperature at 5 and 6 a.m. due to low dew point temperatures. Because of the model limitations, the model is not recommended for very dry climates where ambient temperature is higher than 30°C (86°F).

The Aubinet (1994) model depends on measuring vapor pressure and ambient air temperature. In higher air temperature and lower vapor pressure, as in the cases in Figures 8 and 9, the model predicts lower sky temperature compared to the other two models. In the case of moderate air dry bulb and dew point temperatures, the model predicted a larger difference between sky and ambient temperatures during the morning and late hours over the course of the day.
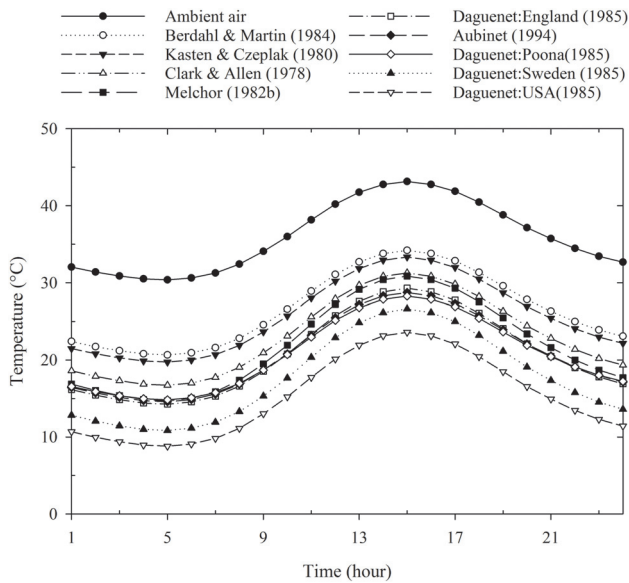

Figure 6 *Comparison of hourly variations between cloudy sky emissivity models and measured ambient air temperature over a 24-hour period.*
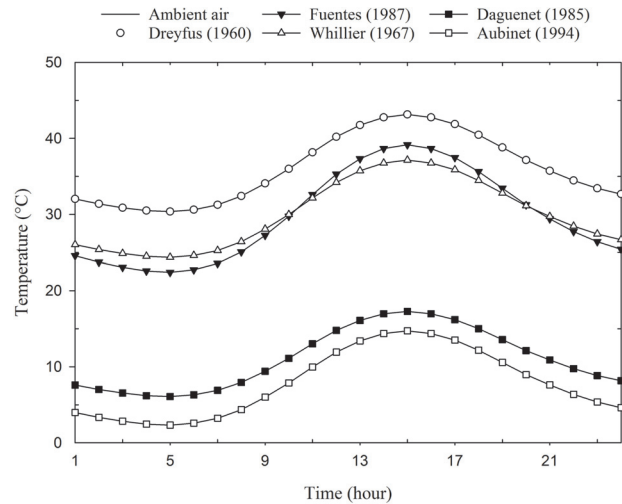

Figure 7 *Comparison of hourly variations between cloudy sky direct models and measured ambient air temperature over a 24-hour period.*

Table 5.   Weather Data for Climate Sites

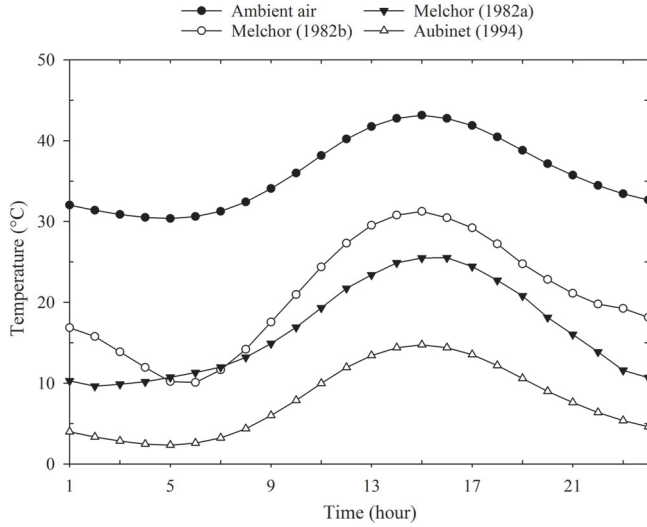| Climate Type	Site	Maximum Air Temperature, °C (°F)	Minimum Air Temperature, °C (°F)	Maximum Dew Point Temperature, °C (°F)	Minimum Dew Point Temperature, °C (°F)
Extreme hot-dry	Al-Madinah, Saudi Arabia	43.33 (110)	30.50 (87)	5.00 (41)	−5.55 (22)
Hot-dry	Phoenix, AZ	40.00 (104)	27.22 (81)	17.77 (64)	9.44 (49)
Hot-humid	Houston, TX	32.77 (91)	23.38 (74)	23.89 (75)	21.11 (70)
Moderate	Chicago, IL	27.77 (82)	18.33 (65)	18.88 (66)	13.33 (56)

Figure 8 *Sky temperature variations using three sky models from literature under extreme hot-dry climate conditions.*

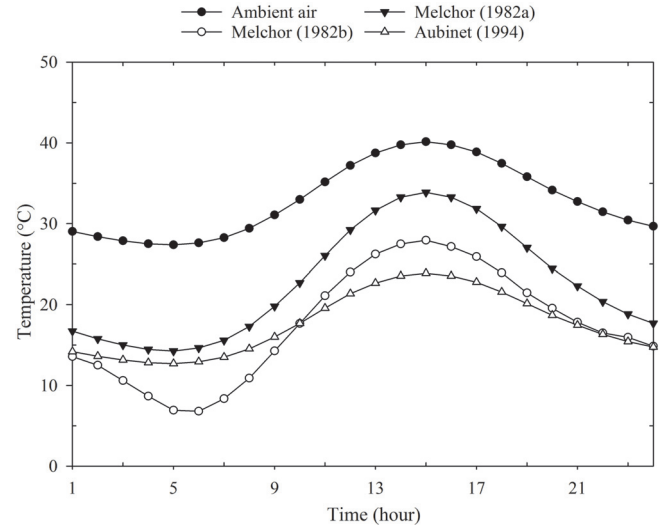**Figure 9** *Sky temperature variations using three sky models from literature under hot-dry climate conditions.*

SKY COOLING LOAD VARIATIONS

To demonstrate the influence of the effective sky temperature on the radiative heat exchange, selected sky temperature models over a 24-hour period were tested in the extreme hot-dry climate of Al-Madinah, Saudi Arabia. A typical horizontal surface consisting of 150 mm (5.9 in.) of reinforced concrete and a layer of plaster attached to the inside of the surface was selected. Three different sky temperature models were selected to cover the area of the existing sky temperature models prediction. The models by Dreyfus, Angstrom, and Daguenet were used. Dreyfus's (1960) and Angstrom's (1918) models are two extreme sky temperature models, while the Daguenet's (1985) Sweden model is considered to be an average estimate of the sky temperature. Results are presented in Figure 12. The daily average sky cooling loads were found to be 293.9, -3828.5, and -1849.9 W-hr/m^2 (93.2, -1213.6, -586.4 Btu/ft^2) respectively. It is interesting to see that the peak sky cooling effect occurs at midday; however, since the peak solar radiation absorbed happens at midday as well, the cooling sky effect is not as apparent. This example demonstrates how significantly different the sky cooling load can be, and thus the impact on cooling load calculations, with different sky effective temperatures.

It should be noted that for cloudy sky conditions, the sky cooling effectiveness is reduced since the sky temperature more closely approaches the ambient temperature. Although roof thermal insulation is essential to proper building performance, it may hinder the singular benefit of sky cooling. Furthermore, sky radiation exchange during totally cloudy conditions could, in some select cases, result in a heat gain to the building. And, in the winter months, the sky cooling effect become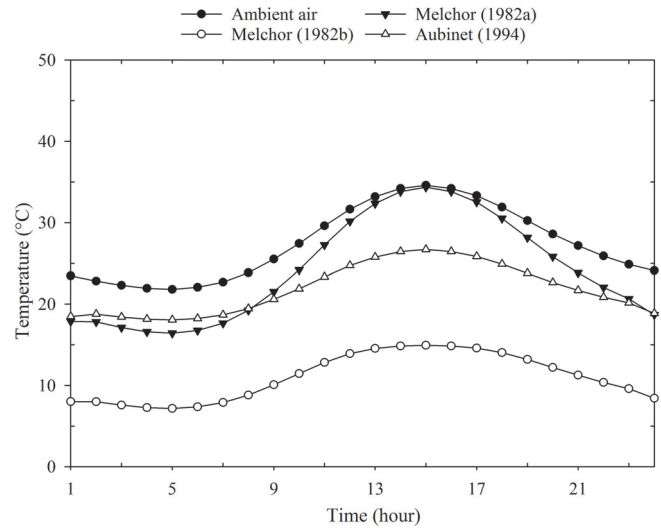s unfavorable. All of these factors emphasize the importance of accurate predictions of sky longwave radiation heat exchange.

Figure 10 *Sky temperature variations using three sky models from literature under hot-humid climate conditions.*

CONCLUSIONS

Several sky temperature models, including clear and cloudy sky models, have been reviewed. Selected sky temperature models were also investigated with different climate condition types. The effect of sky cooling on a horizontal surface was shown, including hourly sky cooling variations with selected sky temperatures models over a 24-hour period.
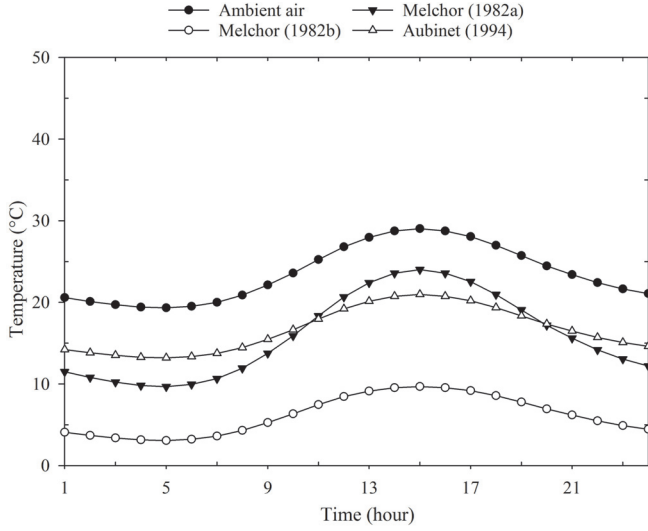
Figure 11 *Sky temperature variations using three models from literature under moderate climate conditions.*
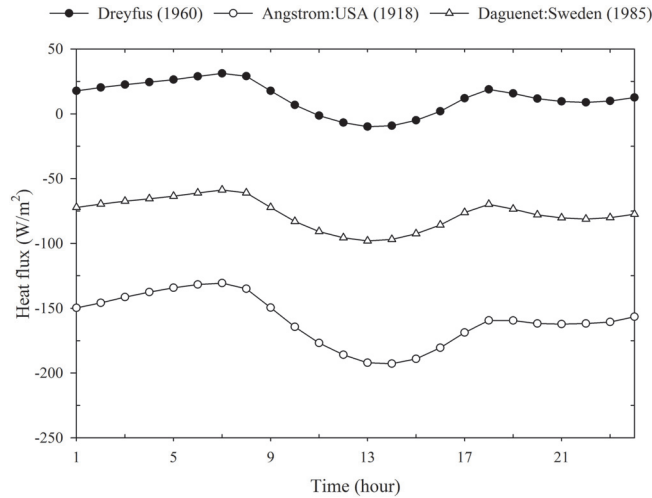

Figure 12 *Hourly sky radiation exchange over a 24-hour period.*

Although the sky temperature models were based on site-specific collected data for a variety of factors, each was presented as a simple algebraic correlation. Among all the sky temperature models, Garg (1982), Swinbank (1963), Dreyfus (1960), and Whillier (1967) are considered the simplest because they are a function of only the ambient air temperature. By using these models, the effective sky temperature can be easily calculated. However, using simple sky models may cause unnecessary errors in estimating the sky temperature. Models such as Melchor (1982b) and Daguenet (1985) account for many factors that strongly affect the sky temperature.

Generally, current sky effective temperature models vary greatly in both form and complexity. It was found that the simplest models were the ones most often utilized. Because there are few locations with a representative sky temperature model, the literature leads to varying results. Therefore, knowledge of current clear and cloudy sky temperature models including their assigned uses (such as a data range, period of collections, proper model location and climate condition) helps in finding a suitable model for a selected site. Furthermore, there is a need for additional data and research that captures additional variables and lead to better sky temperature predictions, for example, improved models including factors that capture daily cycles or hourly changes that are independent of location and that account for dust storms or smog beyond cloudiness factors.

NOMENCLATURE

AH	=	absolute humidity, %
C, f	=	sky cloudiness
F_{ss}	=	view factor with respect to sky
H	=	relative humidity, %
M	=	roof multiple layers
N	=	opaque sky cover
K_0	=	clearness index
P_v	=	vapor pressure, mbar (except models 25, 34, and 35f, in Pa)
P_{atm}	=	atmospheric pressure, mbar
q_{conv}	=	outside roof heat convection, W/m^2
q_i	=	combined internal heat transfer, W/m^2
q_{sky}	=	sky longwave radiation, W/m^2
q_{solar}	=	absorbed solar radiation, W/m^2
T_{amb}	=	ambient air temperature, K
T_{dp}	=	dew point temerature, °C (except model 11a, in K)
T_{sky}	=	sky effective temperature, K
$T_{x=L}$	=	outside roof surface temperature, K
Z	=	site elevation, m
$k_{1...M}$	=	roof layers thermal conductivities, W/m·K
$L_{1...M}$	=	roof layers thickness, mm
$c_{1...M}$	=	roof layers thermal capacities, J/kg·K

Greek

$\rho_{1...M}$	=	roof layers densities, kg/m^3
ε	=	roof outside surface emissivity
ε_{sky}	=	sky effective emissivity
σ	=	Stefan-Boltzmann constant, W/m^2·K^4

REFERENCES

Al-Sanea, S.A. 2000. Evaluation of heat transfer characteristics of building wall elements. *Journal of King Saud University* 12(1):285–313.

Al-Sanea, S.A. 2002. Thermal performance of building roof elements. *Building and Environment* 37(7):665–75.

Angstrom, A. 1918. A study of the radiation of the atmosphere. *Smithson. Inst. Misc. Coll.* 65(3):159–61.

ASHRAE. 1989. *ASHRAE Handbook—Fundamentals*. Atlanta: ASHRAE.

ASHRAE. 2013. *ASHRAE Handbook—Fundamentals*. Atlanta: ASHRAE.

Aubinet, M. 1994. Longwave sky radiation parameterizations. *Solar Energy* 53(2):147–54.

Berdahl, P., and R. Fromberg. 1982. The thermal radiance of clear skies. *Solar Energy* 29(4):299–314.

Berdahl, P., and M. Martin. 1984. Emissivity of clear skies. *Solar Energy* 32(5):663–64.

Berger, X., D. Buriot, and F. Garnier. 1984. About the equivalent radiative temperature for clear skies. *Solar Energy* 32(6):725–33.

Bliss, R. 1961. Atmospheric radiation near the surface of the ground: a summary for engineers. *Solar Energy* 32(5):103–20.

Cavelius, R., C. Isaksson, E. Perednis, and G. Read. 2005. *Passive cooling technologies*. Vienna: Austrian Energy Agency.

Centeno, M. 1982. New formulae for the equivalent night sky emissivity. *Solar Energy* 28(6):489–98.

Chen, B., D. Clark, J. Maloney, W. Mei, and J. Kasher. 1995. Measurement of night sky emissivity in determining radiant cooling from cool storage roofs and roof ponds. *Proceedings of the 20th National Passive Solar Conference, Minneapolis, MN, US,* 20:310–313.

Chen, B., Kasher, J., Maloney, J., Girgis, G., Clark, D. 1991. Determination of the clear sky emissivity for use in cool storage roof and roof pond applications. *Proceedings of the American Solar Energy Society Annul Meeting, Denver, CO, US.*

Chesné, L., T. Duforestel, J.J. Roux, G. Rusaouën, and I.L. Cethil. 2011. Exploitation of the environmental energy resources: indicators and design strategies. *Proceeding of the 12th Conference of the International Building Performance Simulation Association, Sydney, Australia,* 2672–9.

Clark, G., and C. Allen. 1978. The estimation of atmospheric radiation for clear and cloudy skies. *Proceedings of 2nd National Passive Solar Conference (AS/ISES), Philadelphia, PA, US,* 2:675–8.

Clark, G., F. Loxsom, C. Allen, and C. Treat. 1985. *Assessment of passive cooling rates and application in the U.S.* DOE Contract DE- AC03-77CS31600.

Cole, R.J. 1976. The longwave radiative environment around buildings. *Building and Environment* 11(1):3–13.

Daguenet, M., 1985. *Les séchoirs solaires: théorie et pratique*. Paris: United Nations Educational, Scientific and Cultural Organization.

Eicker, U., and A. Dalibard. 2011. Photovoltaic–thermal collectors for night radiative cooling of buildings. *Solar Energy* 85(7):1322–35.

Fuentes, M.K., 1987. *A simplified thermal model for flat plate photovoltaic arrays*. Report SAND85-0330. Albuquerque: Sandia National Labs.

Garg, H.P. 1982. *Treatise on solar Energy: Fundamental of solar energy*. Chichester: John Wiley & Sons.

Hottel, H.C., and R.B. Egbert. 1942. Radiant heat transmission from water vapor. *American Institute of Chemical Engineers Transactions* 38:531–68.

Huang, Y., F. Su, D. Seo, and M. Karati. 2014. Development of 3012 IWEC2 weather files for international locations (RP-1477). *ASHRAE Transactions* 120(1).

Idso, S. B. 1981. On the systematic nature of diurnal patterns of differences between calculations and measurements of clear sky atmospheric thermal radiation. *Quarterly Journal of the Royal Meteorological Society* 107(453): 737–741.

Kasten, F., and G. Czeplak. 1980. Solar and terrestrial dependent on the amount of the type of cloud. *Solar Energy* 24(2):177–188.

Khedari, J., J. Waewsak, S. Thepa, and J. Hirunlabh. 2000. Field investigation of night radiation cooling under tropical climate. *Renewable Energy* 20(2):183–93.

Kondratyev, K.Y. 1969. *Radiation in the atmosphere*. New York: Academic Press.

Kuehn, T.H., J.W. Ramsey, and J.L. Threlkeld, J.L. 1998. *Thermal environmental engineering*. 3rd ed. Hoboken, NJ: Prentice Hall.

Martin, M., and P. Berdahl. 1984. Characteristics of infrared sky radiation in the United States. *Solar Energy* 33(3):321–36.

McQuiston, F.C., J.D. Parker, and J.D. Spitler, J.D. 2005. *Heating, ventilating, and air conditioning: analysis and design*. 6th ed. New York: John Wiley & Sons.

Melchor, C.V. 1982a. New formula for the equivalent night sky emissivity. (model A) *Solar Energy* 28(6):489–98.

Melchor, C.V. 1982b. New formula for the equivalent night sky emissivity. (model B) *Solar Energy* 28(6):489–98.

MEPA. 2013. Meteorology and Environmental Protection Agency (Saudia Arabia) www.pme.gov.sa.

Mills, A.F. 1995. *Heat and mass transfer*. 2d ed. Columbus, OH: McGraw-Hill Higher Education.

NOAA. 2014. National Oceanic and Atmospheric Administration's National Weather Service. www.nws.noaa.gov/climate/.

Praëne, J.P., F. Garde, and F. Lucas, F. 2005. Dynamic modelling and elements of validation of a solar evacuated tube collector. *Ninth International IBPSA Conference*, Montreal, Canada, 953–60.

Raman, P.K. 1935. Heat radiation from the atmosphere at night. *Proceedings of Indian Academy of Sciences* 1:815.

Robitzsch, M. 1926. *Arbeiten Observatorium Lindenberg* 15:194.

Saitoh, T.S., and T. Fujino. 2001. Advanced energy-efficient house (HARBEMAN house) with solar thermal, photo-voltaic, and sky radiation energies (experimental results). *Solar Energy* 70(1):63–77.

Sloan, R., J.H. Shaw, and D. Williams, D., 1956. Thermal radiation from the atmosphere. *Journal of the Optical Society of America* 46(7):543–547.

Spitler, J.D. 2010. *Load calculation applications manual.* Atlanta: ASHRAE.

Swinbank, W. 1963. Long-wave radiation from clear skies. *Quarterly Journal of Royal Meteorological Society* 89:339–48.

Tang, R., Y. Etzion, I.A. Meir. 2004. Estimates of clear night sky emissivity in the Negev Highlands, Israel. *Energy conversion and management* 45(11):1831–1843.

Twidell, J.W., and T.D. Weir 2005. *Renewable Energy resources*. 2d ed. Abingdon, UK: Taylor & Francis.

Whillier, A. 1967. *Design factors influencing solar collectors in low temperature engineering applications of solar energy.* New York: ASHRAE.